UNIVERSITY OF GRAZ

Eclipsing Binaries

by

Maike Bauer

01510694

A thesis submitted in partial fulfillment for the
degree of Bachelor Of Science

to the
Institute of Physics

Supervisor: Dr. Thorsten Ratzka

August 2018

Contents

Chapter 1

Introduction

Since the beginning of mankind, humans have looked up at the sky in amazement; perceiving the sight of stars whose light has traveled for hundreds and thousands of years to reach us. As time went on and mankind progressed, amazement grew into curiosity and curiosity is what finally gave rise to science.

The earliest written records of humans observing the sky date back to 2000 BC and were found in the Near East. It was the Babylonians who first developed the mathematical tools necessary to systematically observe the sun and moon as well as other celestial objects. This knowledge was passed on to other civilizations who, little by little, helped establish astronomy as the scientific field that it is today. The study of variable stars started out fairly recently in comparison to the study of the night sky in general. Often, variable stars were discovered solely due to chance as opposed to any sort of structured search. Variable star research was significantly impacted and advanced by the development of photography in the late nineteenth century. Once the photographic equipment became sensitive enough, the newly invented technology soon started being applied in numerous scientific fields, among them astronomy. With photographic records of the sky, looking for new variable stars and obtaining more information about already discovered ones became much simpler.

As technology advanced and the number of available tools increased, so did the number of known variable stars. In particular, the discovery and subsequent utilization of semiconducting materials proved to be an invaluable tool for the discovery of variable stars. Without semiconductors, CCD-Chips and other indispensable devices would not exist today. The number of known variable stars has gone from just over 1000 in the early twentieth century to many tens of thousands today. Now, there are many observatories and scientists all over the world dedicated to detecting new variable stars as well as classifying and explaining the inner processes at work in already known ones.[1]

In a way, one could say that all stars are variable to some extent. Even our Sun is subject to periodic changes in activity as well as the number of sun spots. Variable stars are an important phenomenon since the details of their variability reveal a lot about the stellar properties. Eclipsing binaries were chosen as the subject of this thesis, because they are particularly valuable in terms of the information that one is able to derive from the measured data. Additionally, systems consisting of two stars are a fairly common occurrence; hence it is important to study them closely, if we truly want to be able to understand the rules that govern the universe.

If we want to be able to draw conclusions about a star's properties, light curves recorded by many different observers have to be analyzed and compared to each other. Large-scale observation missions, such as the well-known Kepler space observatory, further highlight how important cooperation between scientists is for the study of variable stars.

Chapter 2

Basics

Observing and understanding the properties of stars is particularly important, because as far as we know, finding life is unlikely on planets who orbit stars that do not meet certain criteria. Additionally, stars are primarily responsible for the creation of all elements heavier than helium, which again, is necessary for life to form.[2]

2.1 Spectrum

Many of a star's properties are best computed by performing spectral analysis on the observed starlight. Usually, stars emit what is called an absorption-line spectrum which is generated by the stellar atmosphere. The underlying, dense layers on the other hand, emit a continuous spectrum. Absorption lines are characteristic for certain elements and thus allow conclusions to be drawn about the composition of the stellar atmosphere.[1]

2.2 Temperature

It is also possible to gather information about a star's temperature from its absorption lines. The atoms present in the atmosphere are of course sensitive to temperature and density. At low temperatures, atoms are able to form molecules which in turn show up as molecular absorption lines in the spectrum. At higher temperatures, chemical bonds break up and atoms no longer form molecules; some electrons may enter an excited, high-energy state or the atoms might even become ionized. All of the aforementioned factors influence the absorption line spectrum and by measuring the occurrence and strength of the lines, one can infer the star's temperature.[1]

There are of course other methods to estimate the temperature. They all involve the star's photometric properties in one way or another. Depending on which method is used, different types of temperatures are the result. One could, for example, compare the measured intensity of the star's radiation with that of a black body of known temperature and identical size. This leads to the so-called effective temperature. The star's color can also be used to gather the desired information. In this context, the Johnson-system of filters is often used. The letters it uses (U, B and V) stand for ultraviolet, blue and visual. Each name corresponds to the wavelength range that the filter transmits. The magnitude differences that one measures when applying two different filters to the same star, e.g. B-V, correlates with the color and serves as proxy for the temperature of the star, which is why this temperature estimate is called color temperature.[3]

2.3 Magnitude and luminosity

A star's luminosity L depends on its surface area A and its effective temperature T. The connection between these variables is described by the Stefan-Boltzmann law:

$$L = 4 * \pi * r^2 * \sigma * T^4$$

[3]

In the equation above, r denotes the star's radius and σ is the Stefan-Boltzmann constant. The luminosity is measured in Watts and represents the amount of energy a star emits each second. When describing variable stars, the average power is often used. There are, however, other useful ways of specifying a star's brightness.

One is the apparent magnitude m. The magnitude system is a logarithmic scale that divides celestial objects into different categories based on their apparent brightness. Originally, the categories ranged from 1 to 6, with - as later defined - an object of magnitude 1 being 100 times brighter than an object of magnitude 6. The magnitude system had to be expanded since then to allow fainter as well as brighter objects to be categorized. It is also possible for celestial objects to have negative apparent magnitudes. The defining equation is:

$$m_1 - m_2 = -2.5 * log(\frac{I_1}{I_2})$$

In this equation, m_1 and m_2 represent the magnitudes and I_1 and I_2 denote the fluxes of the stars. The system was originally defined with the wavelength range visible to the

human eye, but can be applied to all other wavelength ranges. The apparent magnitude of a star depends on the spectrum it emits. As already mentioned in the previous section, the Johnson photometric system has established itself as a measurement standard. When calculating the magnitudes of stars, not only the filter but also the detector used to observe the object has to be taken into account. This is best done by measuring standard stars with well known magnitudes in a specific filter.

Based on the apparent magnitude, the absolute magnitude M of a star is defined as the apparent brightness it would have, if it were at a distance of 10 parsecs from the observer. The absolute magnitude was introduced to allow direct comparisons between different stars' brightness, no matter how far away from the earth they are located. This means that the absolute magnitude is a direct measure of the star's intrinsic brightness. The magnitude can also be converted to physical units ($W/m^2/A$). [1]

2.4 Mass

Out of all possible parameters, a star's size, and in extension its mass, has the most significant influence on its other properties. The mass governs the star's evolution and eventually determines whether it will turn into a white dwarf, neutron star or black hole at the end of its life cycle.

Stellar masses can only be determined through a limited number of methods; most easily by observing binary systems and applying Kepler's third law:

$$M_1 + M_2 \propto \frac{a^3}{P^2}$$

In this equation, M_1 and M_2 denote the masses of the individual stars, a is the length of the system's semi-major axis and and P stands for the orbital period.

Usually, only the sum of the individual masses can be determined. If an astrometric reference star is present, i.e. if the motion of the stars can be absolutely measured, the individual masses can be calculated. This is, however, a very time-consuming process. [1]

Chapter 3

Variable Stars

3.1 Types

There are many different types and subtypes of variable stars and although an official system of classification is in place, it is far from complete or ideal. The feature that all variable stars have in common is a change in brightness. The underlying mechanisms, periods of variability as well as changes in magnitude, however, differ greatly between different kinds of variables.[1]

In general, variable stars can be separated into two large groups: Intrinsic and extrinsic variables. For intrinsic variables, the variations occur in response to physical changes in the star itself, while extrinsic variables change in brightness due to some external event, e.g. eclipse of one star by another. Variable stars can be further divided into five categories that classify them according to the process responsible for their variability:

- Pulsating variables
- Cataclysmic variables
- Eruptive variables
- Eclipsing binary stars
- Rotating stars

Since this thesis' focus will be on eclipsing binary variables, the explanations for the other types of variables will be kept brief.

Pulsating, cataclysmic, and eruptive variables belong to the intrinsic category. Eruptive and cataclysmic variables both have occasional violent outbursts. While these occur due

to processes on the surface for eruptive variables, thermonuclear reactions are responsible for the variability of cataclysmic variables. Pulsating variables, on the other hand, vary in brightness due to expansion and contraction of the stars' outer shells. The star may remain spherical or change its shape during this periodic process.

The variability of eclipsing binaries and rotating stars is extrinsic in nature. Rotating stars exhibit irregularities, e.g. dark spots or patches, on their surface. The brightness depends upon which side of the star currently faces the observer. As the name suggests, eclipsing binaries are binary star systems whose overall brightness varies when one star eclipses the other. [4]

3.2 Eclipsing binaries

3.2.1 Mechanisms and classification

First of all, it is important to note that while all eclipsing binary stars are part of a binary star system, not all binary star systems are eclipsing binaries. Some binary stars are what is referred to as a wide binary system. In such systems, the stars that orbit each other are relatively far apart making observations of eclipses and resulting changes in brightness unlikely. Eclipsing binaries are usually closer together and seen at an angle relative to Earth that allows an observer to view the system close to edge-on. Even though the change in brightness in eclipsing variables is a result of the geometric configuration of the system, it is possible that interaction, e.g. mass transfer, between two particularly close stars contributes to the variability.

A classification system for eclipsing binaries based on prototype stars is recognized by the General Catalogue of Variable stars and still in use today. The three different subtypes, Algol, Beta Lyrae and W Ursae Majoris, will, however, not be discussed any further at this point, since the modern classification of eclipsing binaries largely relies on the concept of Roche Lobes and Lagrangian surfaces.

If a binary star system contains one special component, e.g. a black hole or a neutron star, it can also be classified based on this concept.[1]

3.2.2 Roche lobes and Lagrangian surfaces

The gravitational potential around an object can be described by a shell-like structure in which each shell represents a surface on which the gravitational potential is constant. These surfaces are called equipotential or Lagrangian surfaces. In single star systems

without any large gravitational distortions, they are approximately spherical. In binary star systems, the two components influence each other and form hour-glass shaped Lagrangian surfaces in addition to the spherical surfaces which still exist close to each star.

The Lagrangian surface within which material is gravitationally bound to the respective star is called a Roche lobe. It follows that the Roche lobe's shape is influenced by both the star's mass and radius. An important parameter that relates to the concept of Roche lobes is the filling factor. As the name suggests, it is a measure for the percentage to which a star fills its Roche lobe. The filling factor does not remain constant over the course of a star's life. In fact, it grows larger as the star expands towards the end of its evolution.

Roche lobes are of significant importance in the analysis of binary star systems. As has already been said, stars naturally expand over time due to fusion in the shells and an increased core temperature and pressure as fusion into heavier elements begins. Once a star is large enough to completely fill out its Roche lobe, matter can be transferred via the inner Lagrangian point L1 to the companion star. Eclipsing variable stars (and binary stars in general) can be classified by the degree to which each star fills out its Roche lobe, as illustrated in Figure 3.1:

Detached binaries None of the components fill their Roche lobe and the tidal force between the components does not have a noticeable impact.

Semi-detached binaries One of the components fills its Roche lobe completely and may already be transferring some of its mass to the other component via the inner Lagrangian point. The other component is not close to filling out its own Roche lobe.

Contact binaries Both components have grown so large that they fill - or even exceed - their respective Roche lobe and are now effectively 'touching' each other. At this stage, mass is transferred between them. The stars may also form an overcontact binary, if there is a shared envelope of matter surrounding them both. [1]

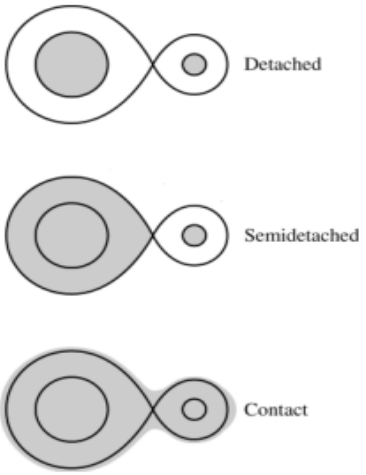

FIGURE 3.1: Schematic drawing of the different types of binary star systems classified according to their Roche lobes. [5]

3.2.3 Period

A system of eclipsing binary stars has two eclipses; a primary and a secondary one. The primary eclipse is the deeper one, meaning that the brighter star, or more precisely the star with the higher effective temperature, gets eclipsed by the darker one thus causing a relatively large drop in brightness. Conversely, the hotter star eclipses the darker one during the shallow secondary eclipse. It is possible for more than two minima to occur in the light curve if a third object passes in front of the binary stars at some point. Furthermore, eclipses may be complete, annular, i.e. ring-shaped, or partial.

A period is the duration between two successive primary or secondary eclipses. For eclipsing binary systems, the found period is usually quite short. It ranges from 0.25 to 10 days but systems with periods of multiple decades have been observed as well, although they are rare.

Period changes in close binary systems are common as mass transfer often occurs between the stars. When mass is transferred, the total mass as well as the angular momentum of the system remain constant but the distance between the components changes. If the stars are particularly close, the effects of tidal effects may contribute to a change in period as well.[1]

3.2.4 Further effects impacting the light curve

It is important to observe eclipsing binary systems, since the presence of two stars makes it easier to accurately determine many stellar properties such as mass or diameter. There

are, however, some common issues that can complicate the analysis.

One such effect is limb darkening. Limb darkening is caused by the fact that the brightness of a star decreases further away from the center. This is because one can see the deeper, hotter layers if the central part of the star is observed, but only the cooler, outermost layers when viewing the limb of the star. When measuring a star's light curve, limb darkening is responsible for the bowl-like appearance of the eclipses and affects the way that rise and decline of the light curve are shaped.

A similar effect, called gravity darkening, is caused by the tidal forces between the two components of the star system. If they are especially close, the stars will eventually be distorted into ellipsoids. The same effect occurs if a star rotates very fast. The edges of these ellipsoids are cooler than the center and thus have a slight influence on the shape of the light curve. Additional variations can occur, if one or both components of a binary star system have noticeable star spots.

In close systems, reflection must be considered. Some of the radiation from one star will be absorbed and re-emitted by the other, causing shoulders around the secondary eclipse as the effect is most prominent just before and after the cooler star's eclipse.

Additionally, the presence of a third star or the occurrence of partial instead of complete eclipses can significantly complicate the analysis.[1]

Chapter 4

Image processing

When working with a CCD camera, it is important to note that a variety of systematic errors can occur and significantly influence the measured data. In order to minimize these errors, some data reduction is typically necessary. In the following section, a brief overview of possible systematic inaccuracies and the methods used to minimize their impact will be given. Additionally, the telescope and filters that were used for the observations will be discussed.

4.1 Telescope and filters

All observations were conducted at Lustbühel Observatory Graz. The 50cm-telescope of Cassegrain type (see Figure 4.1) was used. Further specifications are listed in Table 4.1. An STF-8300M camera was mounted on the telescope. It is monochromatic and its chip has 3326 x 2504 pixels. The camera provides a field-of-view of about 14 arcmin x 10.5 arcmin.[6]

type	Cassegrain
aperture	500 mm
optical diameter primary mirror	500 mm
optical diameter secondary mirror	175 mm
focal length	4500 mm
back focus	410 mm
f-ratio	f9
field-of-view of the telescope	61 arcmin

TABLE 4.1: Specifications of the telescope at Lustbühel Observatory Graz.

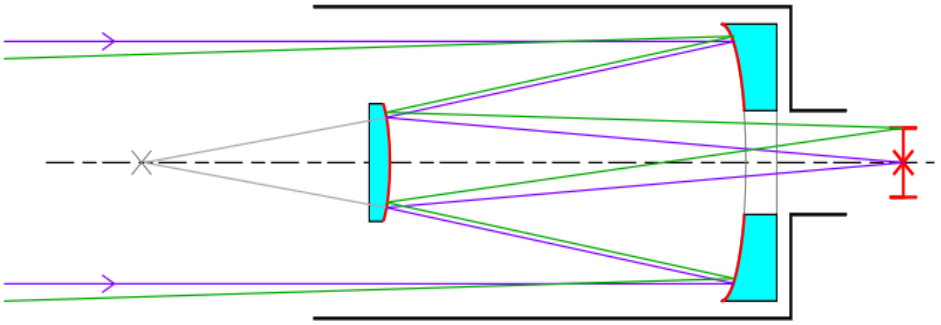

FIGURE 4.1: A Cassegrain type reflecting telescope. The secondary mirror is concave while the primary mirror is convex. [7]

As previously discussed, there are standard sets of photometric filters that are commonly used in astronomy. For the observations presented in this thesis, a V-band filter (visual, from the Johnson system) and an r-band filter (red, from the Sloan system) were used. Information on the bandpasses can be found in Table 4.2. [6]

Filter	λ_{eff}	$\Delta\lambda$
V	547.7	99.1
r	620.4	124.0

TABLE 4.2: λ_{eff} refers to the effective central wavelength, $\Delta\lambda$ is the full width at half maximum. Both quantities are given in nm. [8][9]

4.2 Bias

An integral part of every photometric setup is the so-called CCD-chip. When light hits the chip, the inner photoelectric effect causes electrons to accumulate in the individual pixels. The analog-digital-converter (ADC) translates each pixels charge into a digital signal that can be interpreted by a computer. This process, however, is not free from errors. The process of conversion produces a certain systematic noise that is always present. Additionally, the offset produced by the individual pixels can be determined and corrected. This so-called bias also has a non-systematic component. Some different random errors can occur and alter the bias quite a bit.

To eliminate the bias, creating a master-bias (see Figure 4.3) is necessary. Multiple images are taken without any external light illuminating the chip and an exposure time of zero seconds. Ideally, all that is now visible on these images are the systematic and random errors generated by the aforementioned effects. In the case of the stars observed in this thesis, 10 bias images were taken and averaged to create the master-bias. In this process, the median was used instead of the mean to prevent statistical outliers from having an influence on the result. The bias was then subtracted from the images of the eclipsing binaries. [10]

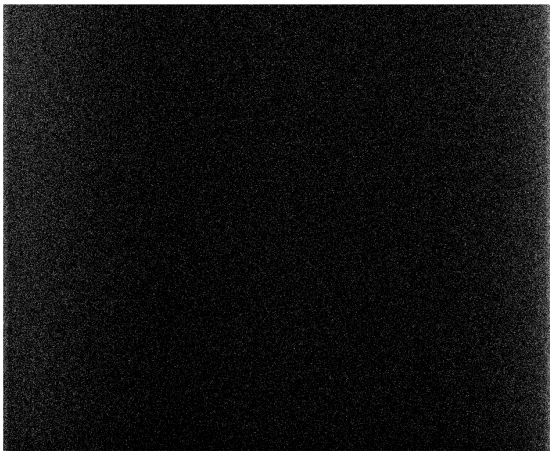

FIGURE 4.2: Image showing a master-bias.

4.3 Dark

During exposure, pixels keep steadily accumulating electrons as a result of dark current. The contribution of this effect primarily depends on the temperature, the exposure time and the characteristics of the pixels. To minimize the consequences of dark current, the

chip has to be kept at a constant, low temperature. Pixels with a particularly high dark current are called hot pixels. A master-dark can be created to eliminate these effects. However, since the equipment was cooled during the measurements and the exposure time was short, this step was not necessary. [10]

4.4 Flat

A flat field is an image taken of an evenly illuminated surface and is meant to show irregularities in the sensitivity of the individual pixels as well as any impurities, e.g. dust particles, on the used filters. For that reason, a flat field must be recorded for each filter. As with the other calibration frames, multiple pictures must be taken and averaged to reduce the influence of outliers. Again, the median is used instead of the mean. Before the master-flat can be created, the bias has to be subtracted from the raw flat frames. Afterwards, it is beneficial to normalize the master-flat by dividing it by its median, so the absolute values of the pixels remain within the same order of magnitude. For this thesis, the flat field chosen was the eastern evening sky at an altitude of about 45 . Such flat fields are called sky flats. Since the exposure time of the flat fields was short, again the dark current was ignored. An image of the master-flats can be seen in Figure 4.3.

The flat field was applied to the science frames after the bias has been subtracted. The science frames were divided by the normalized master-flat. [10]

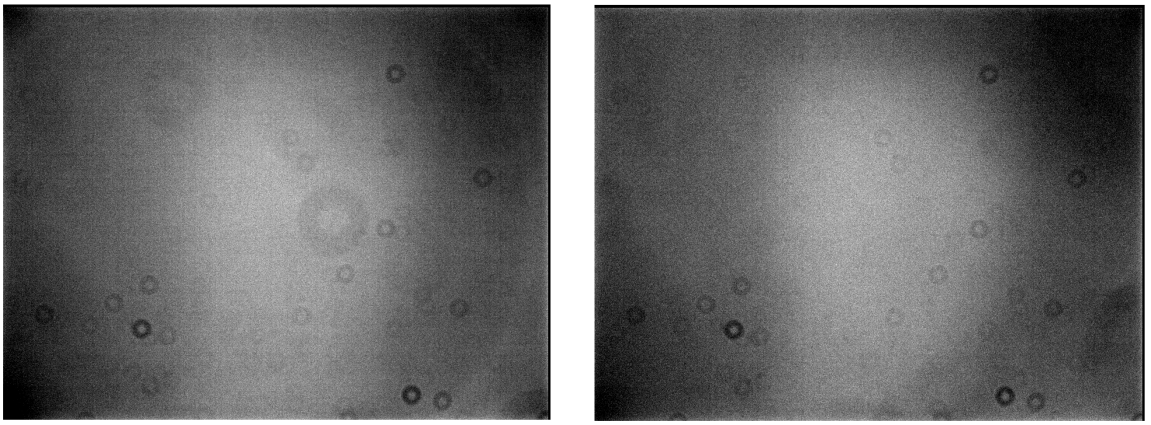

(A) Master-flat when using the r filter. (B) Master-flat when using the V filter.

FIGURE 4.3: Images showing what a master-flat may look like. The master-flat has to be recorded for all filters used.

4.5 Data reduction

After the processes mentioned above had been carried out, the resulting images were further edited by searching for and subsequently eliminating the values of so-called bad pixels.

Aperture photometry was performed on the areas containing the science target and the calibrator star. Before this technique could be applied, a pre-defined section around both objects was cut out. Using an algorithm that utilizes a minimum count rate as well as the full width at half maximum as search criteria, the star and its calibrator could be identified. An even smaller cut-out centered on the found position was then produced and afterwards used for the actual process of aperture photometry (see Figures 4.4 - 4.6 (A)).

A circular aperture with a radius of 18 pixels was placed in the center of the cut-out. The values of the pixels enclosed by this circle were added together. Following that, an annulus, i.e. a ring-shaped region defined by an inner and an outer radius, was centered on the same frame (see Figures 4.4 - 4.6 (B)). The inner radius was set to 18 pixels, the outer radius to 20 pixels. The pixels between the two circles were used to determine the background. The routine then multiplied the average background value of a pixel with the sum of the number of the pixels in the innermost ring and subtracted the result from the counts in the innermost ring.

A calibrator star was used to calibrate the response of the photometric setup and to remove unwanted atmospheric effects, such as extinction. The finished light curves, which can be found in Chapter 5, were obtained by dividing the flux of the science target by the flux of the calibrator. The result was then normalized to 1 and plotted against the minutes since midnight. Times at which no values were recorded were removed from the plot.

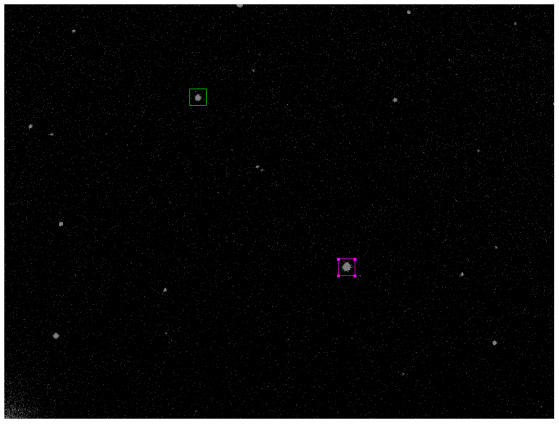

(A) Image of HW Vir (magenta) and its calibrator star (green).

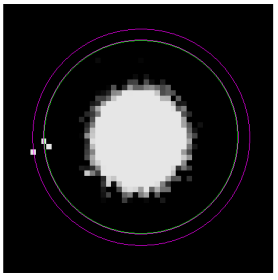

(B) Close-up of HW Vir.

FIGURE 4.4: Images illustrating the process of aperture photometry for HW Vir. The boxes in panel (A) have a size of 50 pixels. The circles used for aperture photometry are pictured in panel (B).

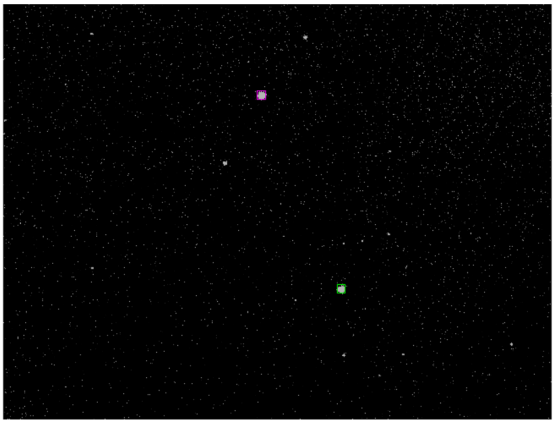

(A) Image of SW Lyn (magenta) and its calibrator star (green).

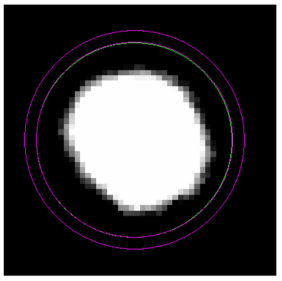

(B) Close-up of SW Lyn.

FIGURE 4.5: Images illustrating the process of aperture photometry for SW Lyn. The boxes in panel (A) have a size of 50 pixels. The circles used for aperture photometry are pictured in panel(B).

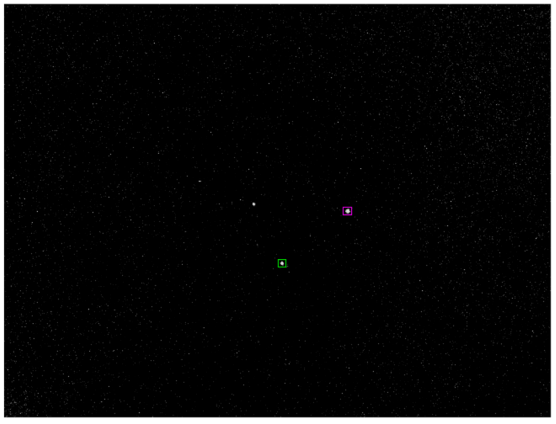

(C) Image of BI CVn (magenta) and its calibrator star (green).

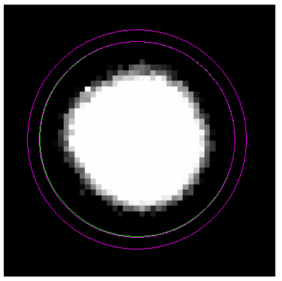

(D) Close-up of BI CVn.

FIGURE 4.6: Images illustrating the process of aperture photometry for BI CVn. The boxes in panel (A) have a size of 50 pixels. The circles used for aperture photometry are pictured in panel (B).

Chapter 5

Evaluation

To be able to draw conclusions about a star's properties, its light curve needs to be studied carefully. The duration of minima as well as their shape reveal important information about the components of binary star systems. To find out whether a model fits a certain star, the recorded light curve can also be compared to a simulated one. For this thesis, three different eclipsing binary stars have been observed. All of the observations were conducted using two different photometric filters. A routine switched between the V- and the r-band filter. The observed systems all have a very short period, usually not more than a few hours.

5.1 HW Vir

HW Vir is a binary star system consisting of a hot subdwarf B star and a cool, small main sequence star. It was observed at Lustbühel observatory on 22.03.2018. Further data concerning the star's parameters can be found in Table 5.1. There, i denotes the inclination and q stands for the mass ratio of the stars. In Table 5.2, important technical data is listed.

T_1	28500 K
T_2	3129 K
r_1	0.197 R_S
r_2	0.181 R_S
L_1	0.9997 L_S
L_2	0.0003 L_S
i	80.97 °
q	0.29
P	0.20

TABLE 5.1: Parameters calculated for the HW Vir system by C. Ibanoglu et al.. The V filter was used in their measurements.[11] The period was calculated by J. H. Wood et. al.. [12]

date	22.03.2018
starting time	22:02 UT
exposure time r-filter	35, 45 s
exposure time V-filter	35, 45 s
duration of measurement	5 h 57 min

TABLE 5.2: Technical data for the observation of HW Vir.

While the stars temperature can be inferred from the methods described in Chapter 2, their respective radii can, for example, be calculated by applying the Stefan-Boltzmann law (see Chapter 2), if the luminosity and the temperature are already known.

To clarify how the parameters mentioned in the table above influence the shape of a binary system's light curve, plots using *nightfall* [13] were compared to the light curves of HW Vir recorded for this thesis. Nightfall allows mass ratio and inclination of the system as well as temperature and Roche lobe filling factor of the respective components to be set. Furthermore, the period, mass of the system as a whole and distance between the components can be chosen. These parameters do, however, not have an influence on the shape of the light curves in the simulation. The luminosity and radius of the respective components mentioned in Table 5.1 can only be set indirectly through the mass ratio or the filling factor.

In Figure 5.1, the two light curves recorded using the different photometric filters can be found. They show a deep primary and a shallow secondary eclipse. This is due to the fact that the second star is much cooler than the first one, resulting in a smaller decline in the system's overall brightness when it is eclipsed. Furthermore, the reflection between the two components can be seen when looking at the shape of the light curve

before and after the primary minimum. In Figure 5.2, the light curves simulated using *nightfall* are shown. The percentage to which the main sequence star fills out its Roche lobe was altered in each comparison plot to demonstrate how the light curve changes as a result of the variation of this parameter. It is important to note that when a star starts filling its Roche lobe, its radius has to increase.

For some of the plots, the flux ratio of the recorded light curves had to be converted to the magnitude difference to be able to compare them to the simulated ones. This was done by applying the magnitude law from Chapter 2. Additionally, the phase parameter used for the simulated graphs had to be converted to the minutes since midnight scale used for recorded light curves. This was done by finding the time stamps that significant points, usually the beginning and end as well as the primary and secondary minimum, would have to have. The times for the data points in between those significant points were then interpolated.

As can be seen in Figure 5.1, the primary minimum of HW Vir is noticeably less deep when using the r-filter. This means that the difference in flux between the science target and the calibrator is larger when using the V-filter.

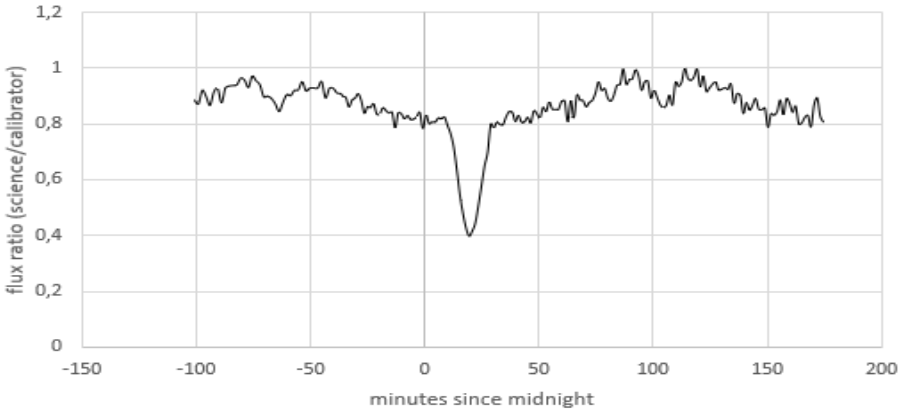

(A) Light curve of HW Vir using the V filter.

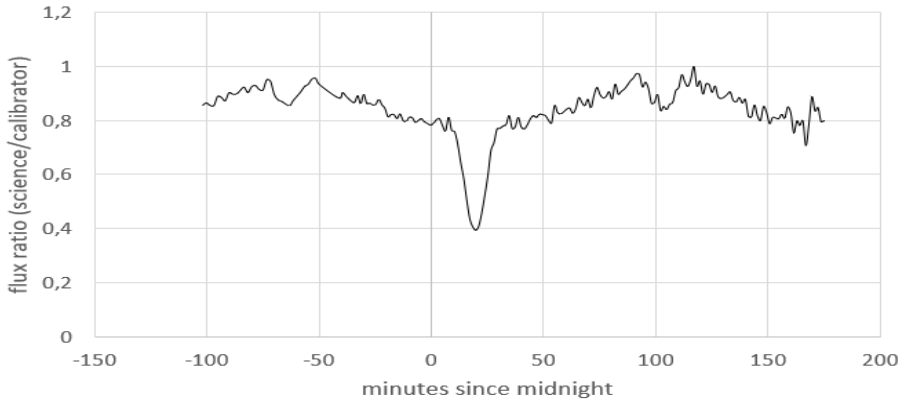

(B) Light curve of HW Vir using the r filter.

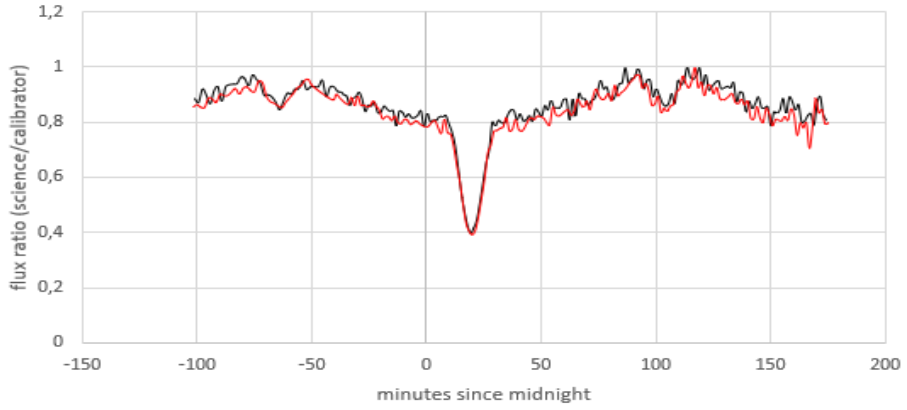

(C) Light curves superimposed on each other (black: V, red: r).

FIGURE 5.1: Graphs showing the two recorded light curves for HW Vir using different photometric filters. A shallow secondary and deeper primary eclipse are visible.

HW Vir is a so-called pre-cataclysmic binary system. In such systems, one (or both) of the components is close to filling out its Roche lobe. In the case of HW Vir, the cool main sequence star is the one currently expanding. The orbital period of the system is

decreasing, and the two stars will be in contact if the period has fallen below a certain threshold. The exact mechanism by which the systems period decreases is still subject of discussion. Both a third body present in the system as well as mass loss through a weak stellar wind have been suggested as a possible reason.[11]

In the graphs shown in Figures 5.2 and 5.3, the effect that the expansion of the main sequence star would have on the light curve becomes obvious. The more the star fills its Roche lobe, the deeper the primary eclipse becomes, and the shallower the secondary eclipse appears in relation to it. The simulated graphs confirm the assumption that HW Vir is a pre-cataclysmic binary system. The graph in which the secondary star fills 80 % of its Roche lobe is the best fit out of the three simulations. However, it is not an exact fit since the primary eclipse is slightly too shallow. The simulated graph in which the secondary star fills its Roche lobe completely does not match the recorded light curve exactly either. This suggests, that the secondary star has a filling factor somewhere between 80 % and 100 %.

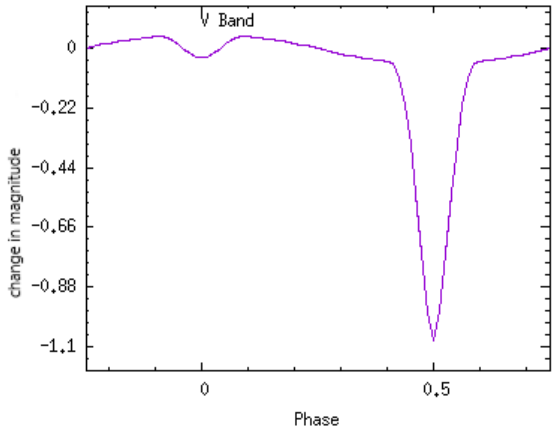

(A) Simulation of the light curve of HW Vir assuming that the cooler star fully fills its Roche lobe.

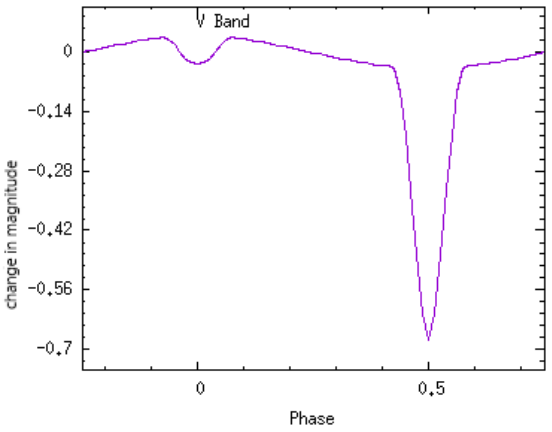

(B) Simulation of the light curve of HW Vir assuming that the cooler star fills 80 % of its Roche lobe.

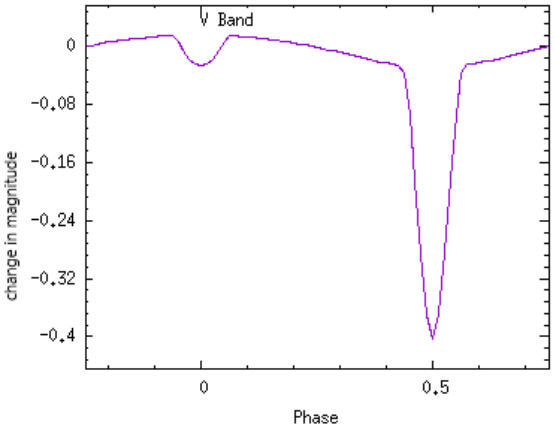

(C) Simulation of the light curve of HW Vir assuming that the cooler star fills 60 % of its Roche lobe.

FIGURE 5.2: Three simulated light curves showing different parameters for the cooler star's Roche parameter. The Roche lobe parameter of the subdwarf remains unchanged (60 %) in all three plots.

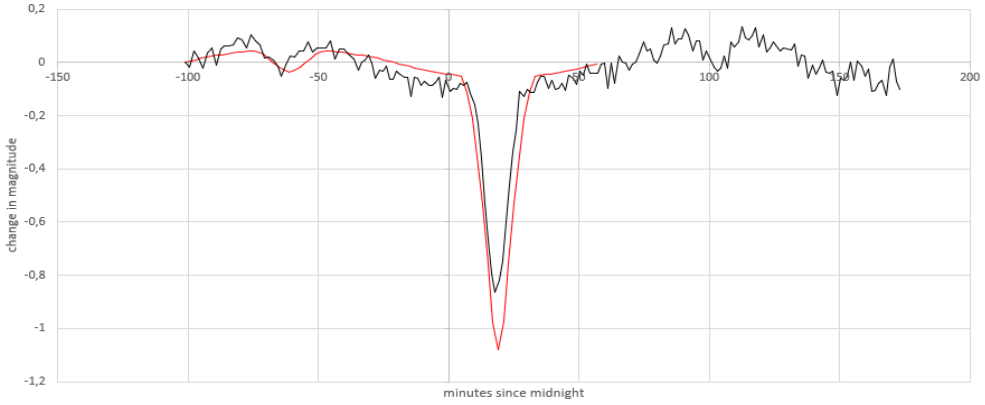

(A) The simulated secondary star fully fills out its Roche lobe.

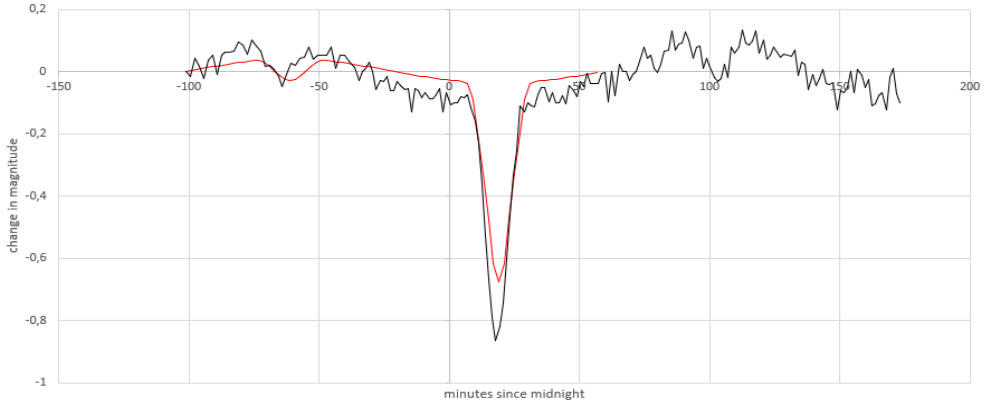

(B) The simulated secondary star fills out 80 % of its Roche lobe.

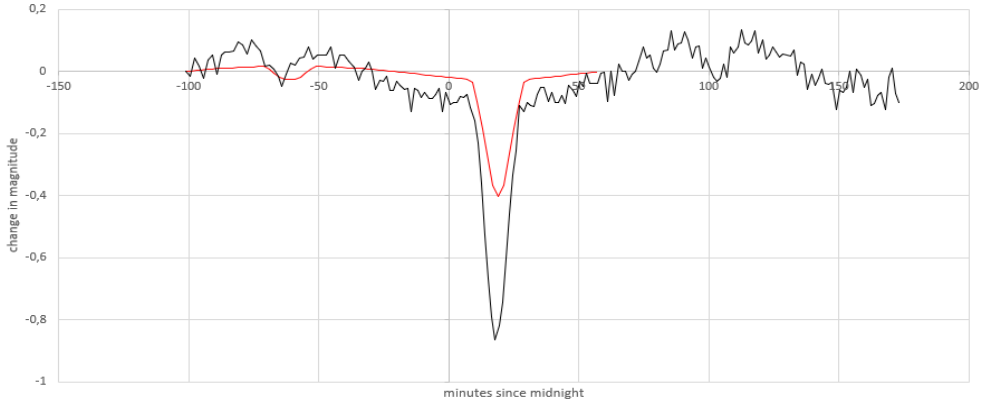

(C) The simulated secondary star fills out 60 % of its Roche lobe.

FIGURE 5.3: Three graphs showing the simulated light curves (red) from Figure 5.2 superimposed on the recorded light curve of HW Vir.

In Figure 5.4, the different Roche lobe configurations that were used for the simulated light curves can be seen again, this time in the form of a graphical representation of the two stars in the HW Vir system. It shows that the more a star fills out its Roche lobe, the larger it becomes. Additionally, if the Roche lobe is fully filled, the star is no longer spherical but appears distorted.

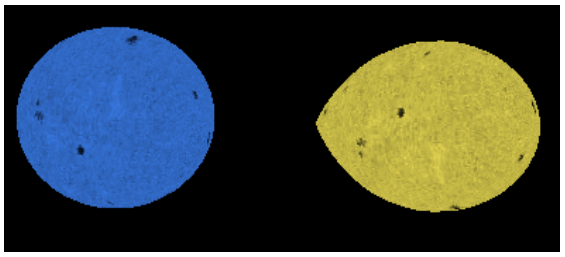

(A) The simulated secondary star fully fills out its Roche lobe.

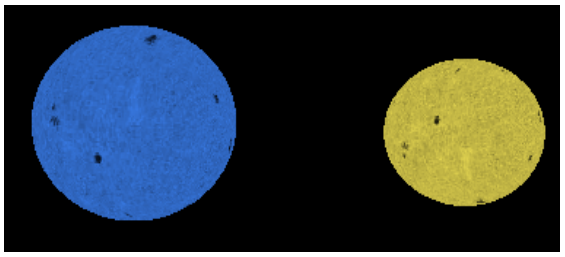

(B) The simulated secondary star fills out 80 % of its Roche lobe.

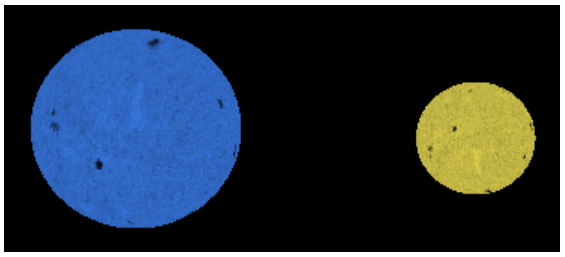

(C) The simulated secondary star fills out 60 % of its Roche lobe.

FIGURE 5.4: Images showing the different percentages to which the secondary star (yellow) fills out its Roche lobe in the simulations.

In the following simulated plots, different values for the system's mass ratio as well as the main sequence star's temperature were used while the other parameters remained unchanged. The results are shown in Figures 5.5 and 5.7. In Figure 5.6, a visual representation of what the different mass ratios look like for HW Vir can be found.

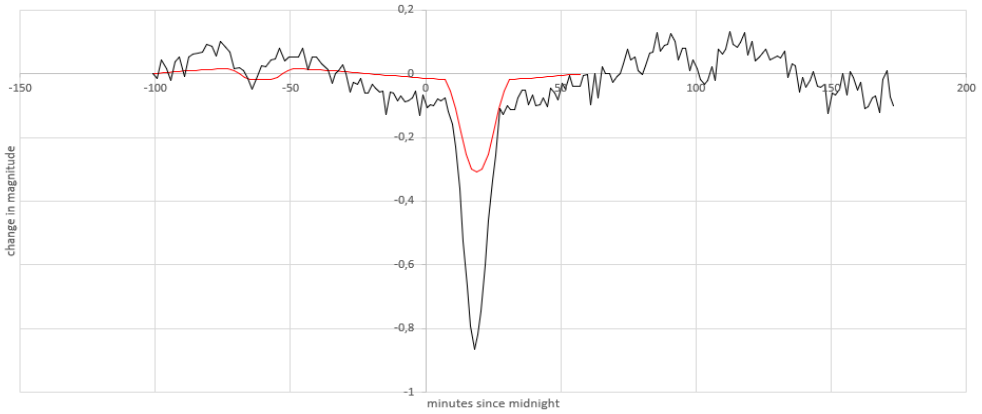

(A) Simulated light curve with a mass ratio of 0.1.

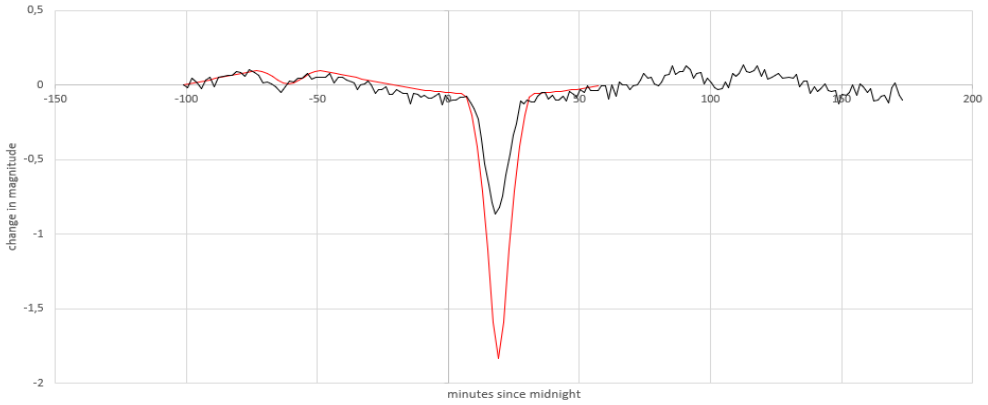

(B) Simulated light curve with a mass ratio of 1.

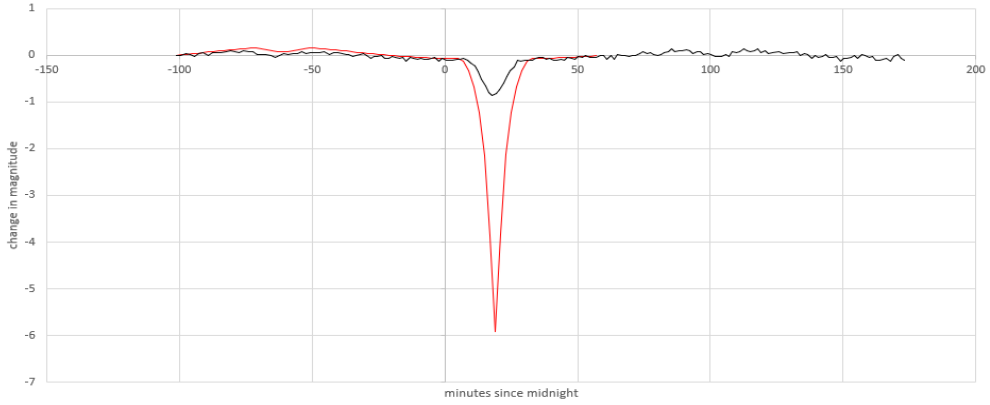

(C) Simulated light curve with a mass ratio of 2.

FIGURE 5.5: Graphs comparing the recorded light curve of HW Vir to simulated light curves (red) with different mass ratios.

As can be seen in the above graphs, the mass ratio of a system influences how deep the primary and secondary minima are. A large mass ratio results in a less massive primary star while the secondary star becomes more massive, leading to a deeper primary and shallower secondary minimum. This is due to the fact that a larger secondary star is able to eclipse more of the smaller primary star since the mass is directly coupled to the

radius of a star by the Roche lobe and the filling factor. The opposite is true if the mass ratio decreases.

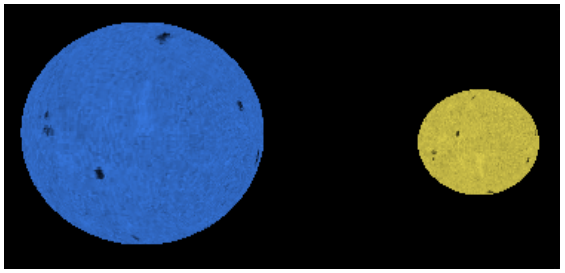

(A) The system at a mass ratio of 0.1.

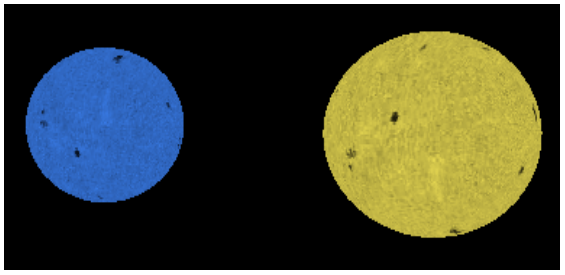

(B) The system at a mass ratio of 1.

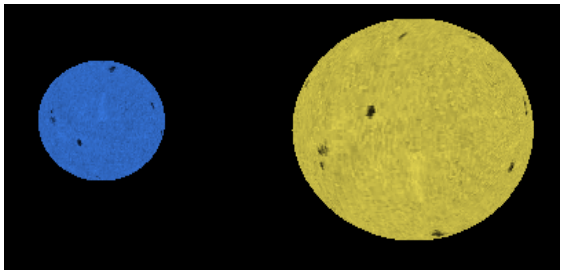

(C) The system at a mass ratio of 2.

FIGURE 5.6: Images showing HW Vir if it had the mass ratios that were used in the simulated light curves in Figure 5.2.

The main sequence star's temperature influences the shape of the light curve quite significantly. Even if the stars have a low flux ratio of 0.1 (see Figure 5.5 (A)), the primary star's comparatively large temperature still results in a much larger change in the system's overall magnitude when it is eclipsed by the cooler star. The depths of the minima become more similar as the difference in the two components' temperature decreases.

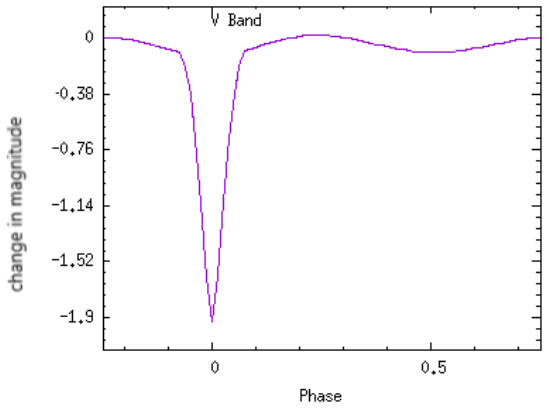

(A) Simulated light curve with $T_2 = 1000$ K.

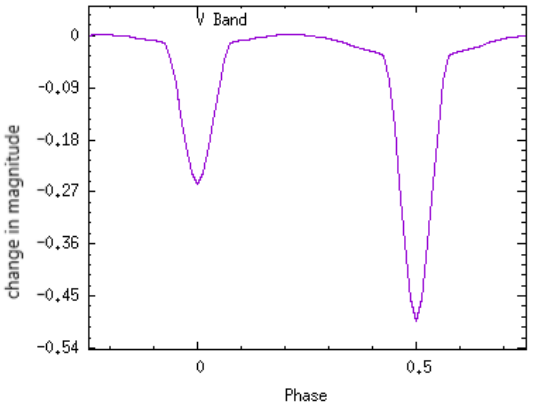

(B) Simulated light curve with $T_2 = 20000$ K.

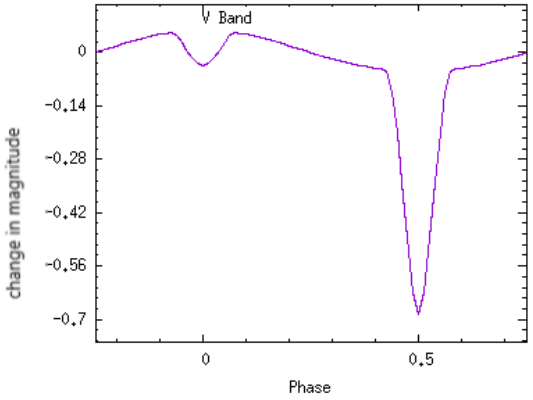

(C) Simulated light curve with $T_2 = 50000$ K.

FIGURE 5.7: Graphs showing the simulated light curve of HW Vir with different temperatures for the secondary star. The original mass ratio of 0.29 was used.

5.2 SW Lyn

SW Lyn is one of the lesser known and analyzed binary star systems. It consists of a hotter and a cooler component. Their precise classification is not yet known. SW Lyn was observed at Lustbühel observatory on 28.02.2018. Further data can be found in Table 5.3. Technical data can be found in Table 5.4.

T_1	6700 K
T_2	4520 K
r_1	1.63 R_S
r_2	1 R_S
L_1	11.13 L_S
L_2	0.78 L_S
i	86.40 °
q	0.35
P	0.6440661 days

TABLE 5.3: Parameters calculated for the SW Lyn system by W. Ogloza et al.. The V filter was used in their measurements and it was assumed that a third body is present. The values in this table were calculated under this assumption.[14] The radius of the two components as well as the period were calculated by M. Vetesnik.[15]

date	28.02.2018
starting time	17:58 UT
exposure time r-filter	30 s
exposure time V-filter	60 s
duration of measurement	7 h 14 min

TABLE 5.4: Technical data for the observation of SW Lyn.

In Figure 5.8, the two light curves recorded using the V and r photometric filters are shown. The light curve of SW Lyn has, as does that of any other binary star system, a primary and a secondary minimum. In Figure 5.8, however, only the deep primary eclipse is visible. The shallower secondary was not observable on the date the observations took place. As is the case with HW Vir, the observed minimum appears to be less deep when using the r-filter.

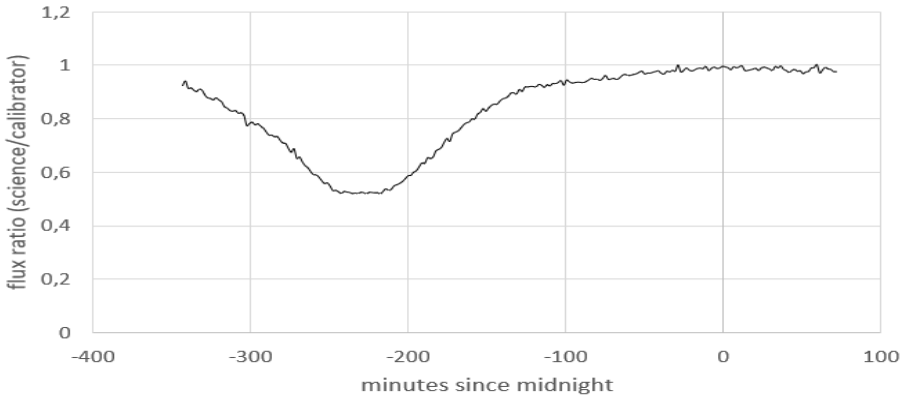

(A) Light curve of SW Lyn using the V filter.

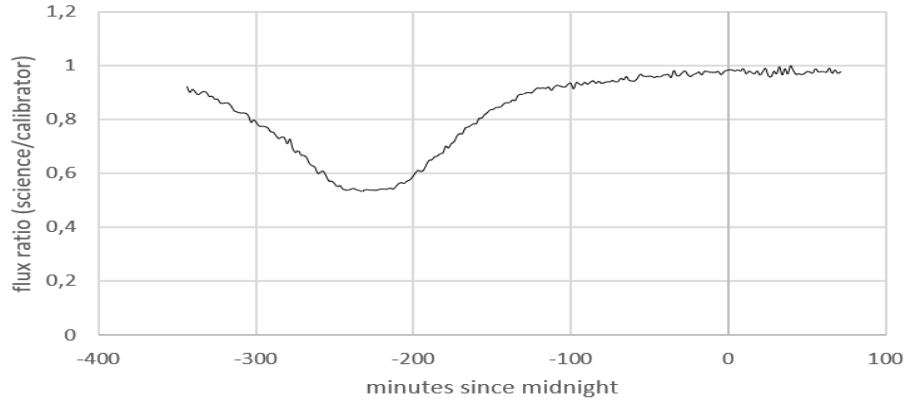

(B) Light curve of SW Lyn using the r filter.

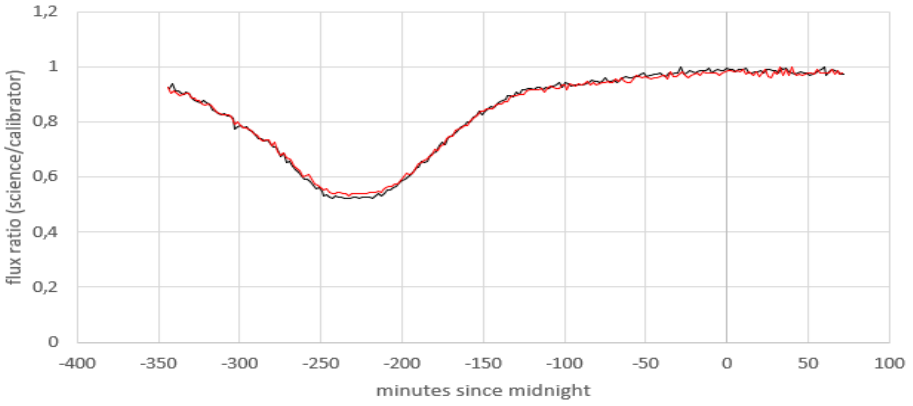

(C) Light curves superimposed on each another (black: V, red: r).

FIGURE 5.8: Graphs showing the two recorded light curves for SW Lyn using different photometric filters. Only the deep primary eclipse is visible.

It was believed that the binary system's orbit has an eccentricity of about 0.11. This assumption led to the belief that SW Lyn must be a detached system. More recently, this has been revised. It was concluded by W. Ogloza et al. that SW Lyn does not have a significant orbital eccentricity and is instead influenced by a third star in the system.

When assuming the presence of a third star, a semi-detached configuration is a better fit.[14]

In Figure 5.9, the simulated light curves are shown. Here, the secondary minimum is visible as well. The percentage to which each star fills out its Roche lobe was changed in each of the three plots. The light curves are compared to the measurement in Figure 5.10. Due to the absence of the secondary minimum in the recorded light curve, it is hard to tell which of the chosen parameters for the Roche lobe fits best. When judging solely by the depth of the primary minimum, the configuration in which both stars fill 80 % of their Roche lobe appears to lead to the best fit. To obtain more meaningful results, observing the secondary eclipse would be necessary.

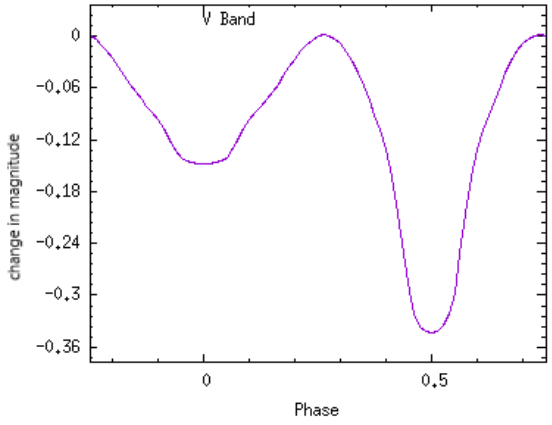

(A) Simulation of the light curve of SW Lyn assuming that the primary star fully fills its Roche lobe and the secondary star fills out 60 % of its Roche lobe.

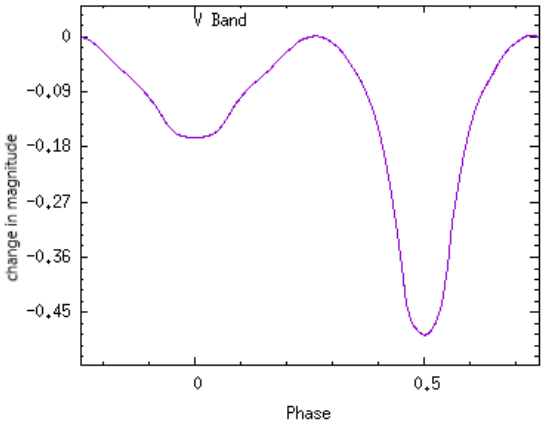

(B) Simulation of the light curve of SW Lyn assuming that the primary star fully fills its Roche lobe and the secondary star fills out 80 % of its Roche lobe.

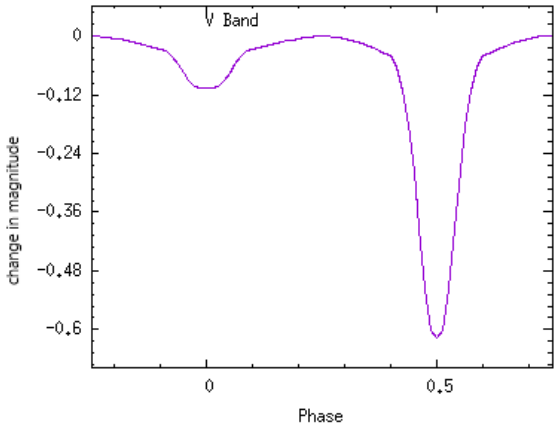

(C) Simulation of the light curve of SW Lyn assuming that both components fill 80 % of their Roche lobe.

FIGURE 5.9: Three simulated light curves showing different parameters for both stars' Roche lobe. The shallower secondary eclipse is visible as well.

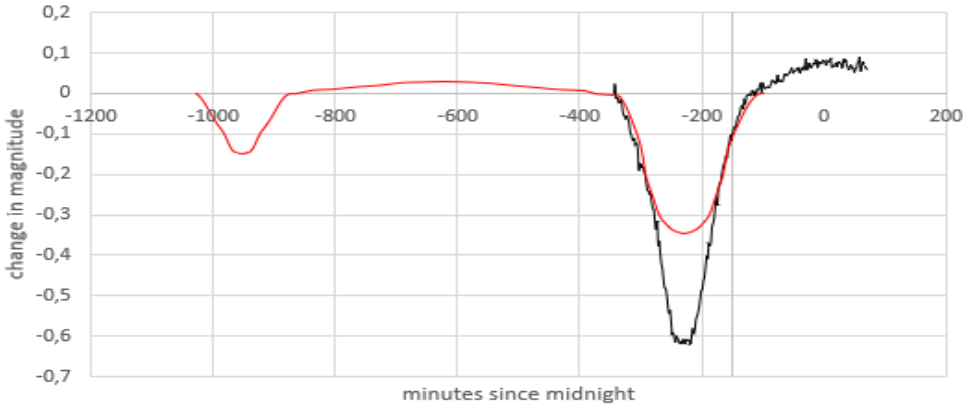

(A) The simulated secondary star fills out 60 % of its Roche lobe.

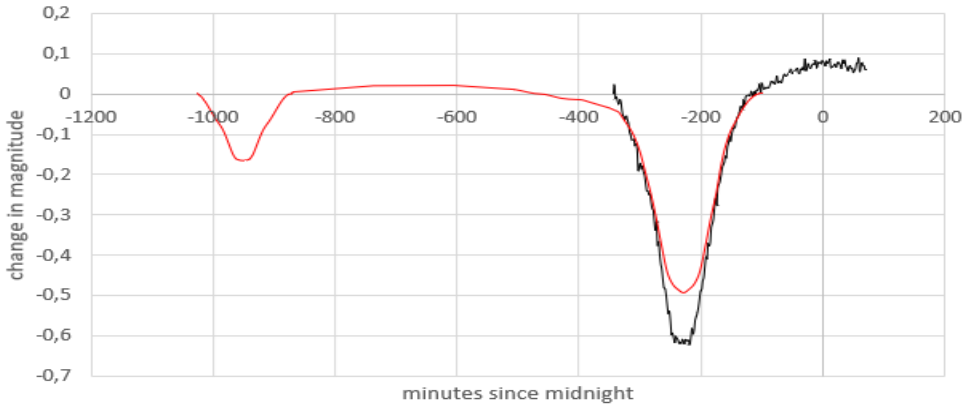

(B) The simulated secondary star fills out 80 % of its Roche lobe.

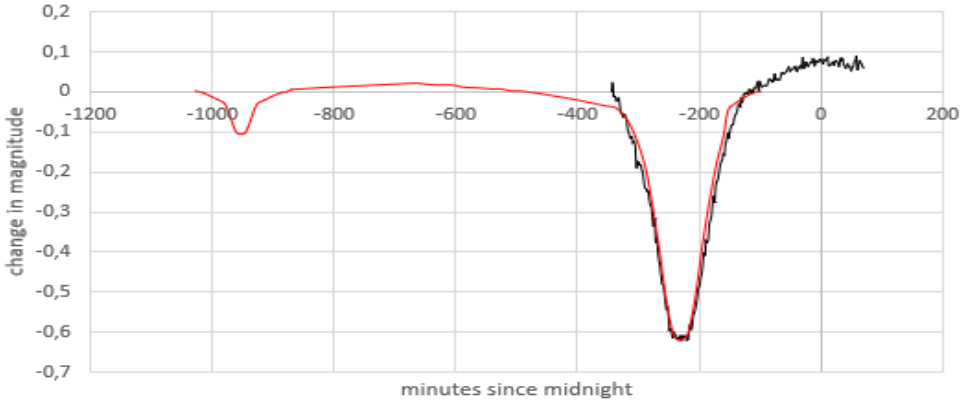

(C) Both of the simulated stars fill out 80 % of their individual Roche lobes.

FIGURE 5.10: Three graphs showing the simulated light curves (red) from Figure 5.9 superimposed on the recorded light curve of SW Lyn.

In Figure 5.11, images depicting the simulated stars with their different Roche lobe configurations can be found.

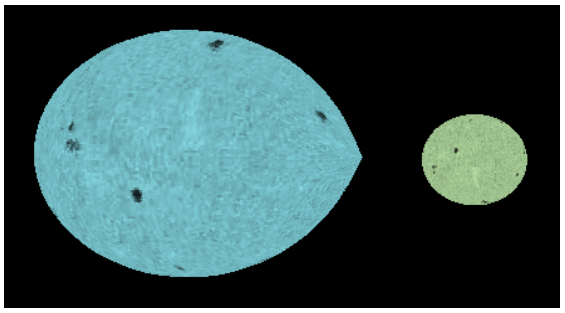

(A) The simulated secondary star fills 60 % of its Roche lobe while the primary star fully fills its Roche lobe.

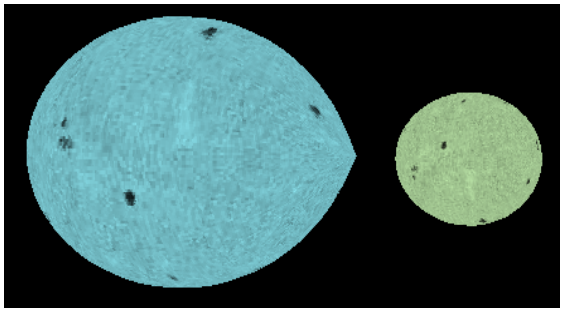

(B) The simulated secondary star fills 80 % of its Roche lobe while the primary star fully fills its Roche lobe.

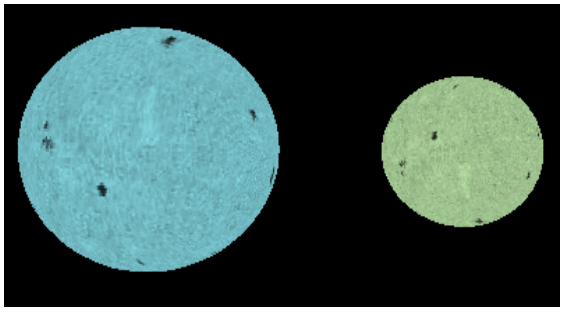

(C) Both of the simulated stars fill 80 % of their Roche Lobe.

FIGURE 5.11: Images showing the different percentages to which the secondary star (green) fills its Roche lobe in the simulations.

5.3 BI CVn

BI CVn is an overcontact binary system undergoing partial eclipses. The two components are almost identical in temperature as a result of their shared envelope, although the second star is much more luminous due to its larger radius. The orbital period has shown significant variations over the past few decades. It is assumed that this is due to a large star spot on the secondary component. A star spot would also explain the difference between the height of the maxima over the years.[16] BI CVn was observed at Lustbühel observatory on April 17th, 2018. Further data can be found in Table 5.5, the technical data is in Table 5.6.

T_1	6170 K
T_2	6093 K
r_1	0.96 R_S
r_2	1.40 R_S
L_1	1.19 L_S
L_2	2.44 L_S
i	71.28 °
q	0.41
P	0.3841692 days (Demircan, cited in Nelson 2013)

TABLE 5.5: Parameters calculated for the BI CVn system by R. H. Nelson et al.. The V as well as the r filter were used in their measurements. [16]

date	17.04.2018
starting time	18:35 UT
exposure time r-filter	60 s
exposure time V-filter	60 s
duration of measurement	8 h 22 min

TABLE 5.6: Technical data for the observation of BI CVn.

The recorded light curves can be found in Figure 5.12. The primary and secondary minimum are of almost equal depth due to the fact that the two components are in contact with each other and have similar temperatures. This leads to an almost identical depth of the respective minima when using the r- and V-filter (see Figure 5.12 (C)). For the simulated light curve in Figure 5.13, it was assumed that both components completely fill out their respective Roche lobe.

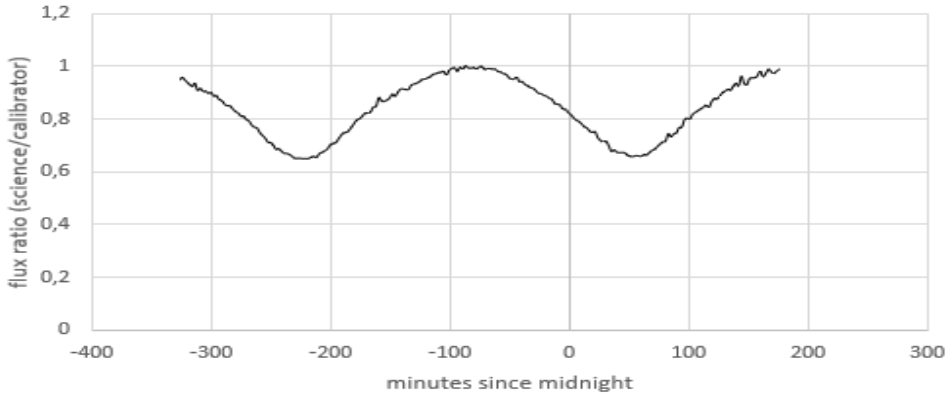

(A) Light curve of BI CVn using the V filter.

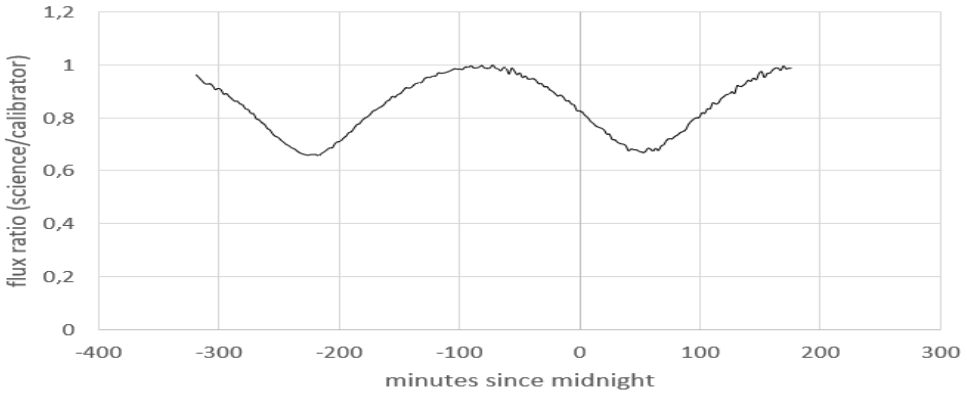

(B) Light curve of BI CVn using the r filter.

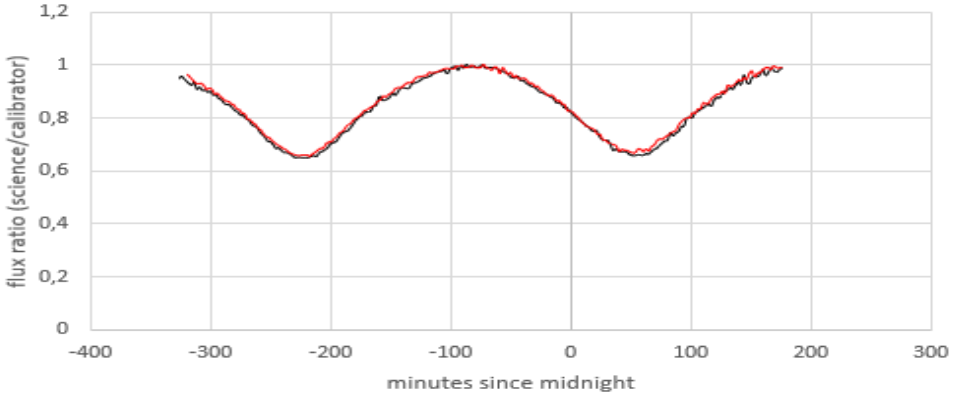

(C) Light curves superimposed on each other (black: V, red: r).

FIGURE 5.12: Graphs showing the two recorded light curves for BI CVn using different photometric filters.

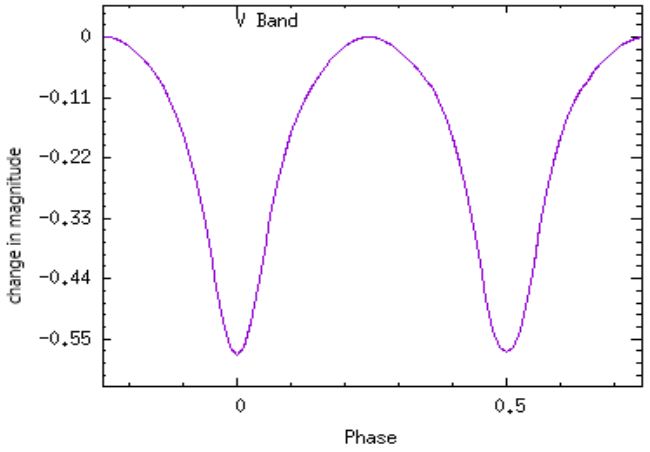

FIGURE 5.13: A simulated light curve showing BI CVn's light curve using the parameters listed in Table 5.5.

Figure 5.14 shows that the simulated curve using the aforementioned parameters fits the recorded curve reasonably well, supporting the well-established notion that BI CVn is a contact system. If the star spots presumably present on BI CVn had been taken into account while simulating the light curve, an even better fit could possibly have been obtained. In Figure 5.15, a visual representation of the system is shown.

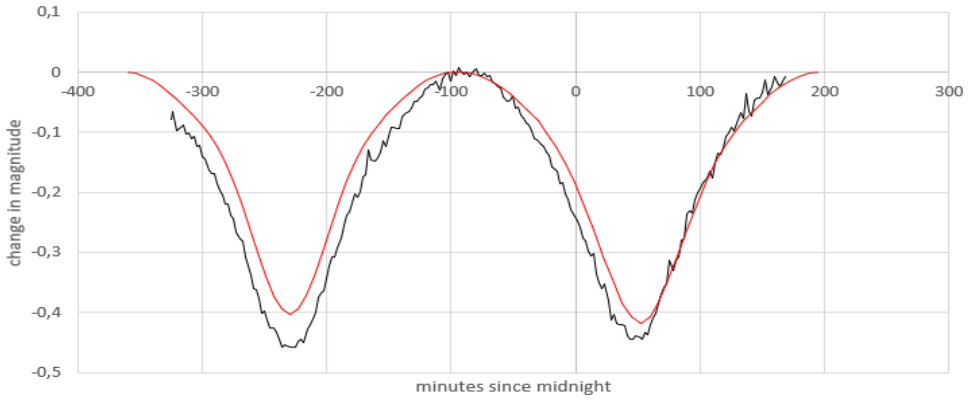

FIGURE 5.14: Graph showing the simulated light curve (red) from Figure 5.13 superimposed on the recorded light curve of BI Cvn.

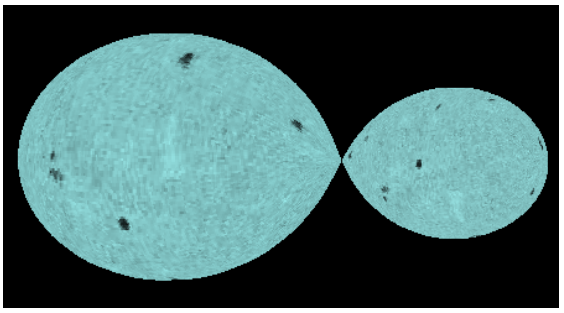

FIGURE 5.15: Image showing the simulated BI CVn system using the parameters mentioned in Table 5.2 and assuming that both components fill out their Roche lobes.

Chapter 6

Conclusion

The aim of this thesis was to observe variable stars and record their light curves in order to gain some insight into this field of astronomy. In total, 4 different binary star systems were observed. Out of those 4 observations, 3 can be considered successful and were presented in this thesis. The fourth observed object, Algol, unfortunately did not show a useable light curve due to the fact that the minimum occurred later than expected. Additionally, finding a appropriate comparison star for Algol proved to be difficult. In general, such observations are also heavily weather-dependent and the planned observation of another eclipsing binary system had to be canceled because of increasing cloud coverage.

Some of the fundamental properties of the stellar systems can be deduced from analyzing the light curves. In order to be able to actually calculate numerical values of certain properties, further analysis would be necessary. The existence of star spots or additional components in the various systems could not be inferred solely from the light curves recorded for this thesis. Observations spanning multiple years are necessary to detect the effects of these irregularities.

The simulated light curves were mostly in accordance with the recorded ones, leading to the conclusion that the parameters derived by the various research groups cited in this thesis are accurate. The use of different parameters for the degree to which each star fills out its Roche lobe lead to a better understanding of how this variable affects the shape of light curves. It was, however, difficult to determine which value for the parameter is the most fitting.

In conclusion, the observations produced the expected results, although further observations are necessary to draw more precise conclusions about the 3 systems' properties.

Bibliography

[1] John R. Percy. *Understanding Variable Stars*. Cambridge University Press, 2007.

[2] Variables: What are they and why observe them? AAVSO Website, 2017. URL `https://www.aavso.org/variables-what-are-they-why-observe-them`.

[3] Arnold Hanslmeier. *Moderne Astrophysik*. bookboon.com, 2015.

[4] Types of variables. AAVSO Website, 2017. URL `https://www.aavso.org/types-variables`.

[5] Max Pettini. Binary stars and type ia supernovae. University of Cambridge Website. URL `https://www.ast.cam.ac.uk/~pettini/STARS/Lecture18.pdf`.

[6] Florian Koller. Stellar reflection nebulae. Bachelor's thesis, University of Graz, 2016.

[7] Wikipedia, August 2014. URL `https://commons.wikimedia.org/wiki/File:Cassegrain_Telescope.svg`.

[8] Johnson-Cousins UBVRI filter curves. Leibniz-Institute website, . URL `http://www.aip.de/en/research/facilities/stella/instruments/data/johnson-ubvri-filter-curves`.

[9] Sloan ugriz filter curves. Leibniz-Institute website, . URL `http://www.aip.de/en/research/facilities/stella/instruments/data/sloanugriz-filter-curves`.

[10] Harald Tomsik. Kalibrierung mittels bias-, dark- und flatframe. URL `http://www.sternwarte-melle.de/index_htm_files/Kalib_1-2.pdf`.

[11] C. Ibanoglu, Ö. Cakirli, G. Tas, and S. Evren. High-speed photometry of the pre-cataclysmic binary HW Virginis and its orbital period change. *Astronomy & Astrophysics*, 2003. doi: 10.1051/0004-6361:20034013.

[12] Janet H. Wood, Er-Ho Zhang, and E. L. Robinson. HW Virginis: a short-period eclipsing binary containing an sdB star. *Monthly Notices of the Royal Astronomical Society*, 1993.

[13] Nightfall. URL `https://www.hs.uni-hamburg.de/DE/Ins/Per/Wichmann/Nightfall.html`.

[14] W. Ogloza, S. Zola, J. Tremenko, and J.M. Kreiner. The analysis of light curves and the third body in the eclipsing binary system SW Lyn. *Astronomy & Astrophysics*, 1998.

[15] M. Vetesnik. Elements for spectroscopic and photometric close binary SW Lyncis. *Astronomical Institutes of Czechoslovakia, Bulletin*, 1977.

[16] R.H. Nelson, H.V. Senavci, . Bastrk, and E. Bahar. BI CVn - A spotted, overcontact, type-W eclipsing binary. *New Astronomy*, 2014.

Symbols

Symbol	Name	Unit
L	luminosity	W
r	radius of star	m
T	temperature	K
m	magnitude	mag
M	mass	kg
I	flux density	W * m^{-2} * Hz^{-1}
a	length of semi-major axis	m
P	orbital period	s
i	inclination	$^\circ$
q	mass ratio $\frac{M_1}{M_2}$	
σ	Stefan-Boltzmann constant	W * m^{-2} * K^{-4}
π	Pi	